Supporting Information

Effects of Cd Diffusion and Doping in High-Performance Perovskite Solar Cells Using CdS as Electron Transport Layer

Wiley A. Dunlap-Shohl[†], Robert Younts[‡], Bhoj Gautam[‡], Kenan Gundogdu[‡] and David B. Mitzi[†§*]

[†] Department of Mechanical Engineering and Materials Science, Duke University, Durham, NC, 27708

[‡] Department of Physics, North Carolina State University, Raleigh, NC 27695

[§]Department of Chemistry, Duke University, Durham, NC 27708

*Corresponding Author Contact Information:

Email: david.mitzi@duke.edu

Tel: (919)-660-5356

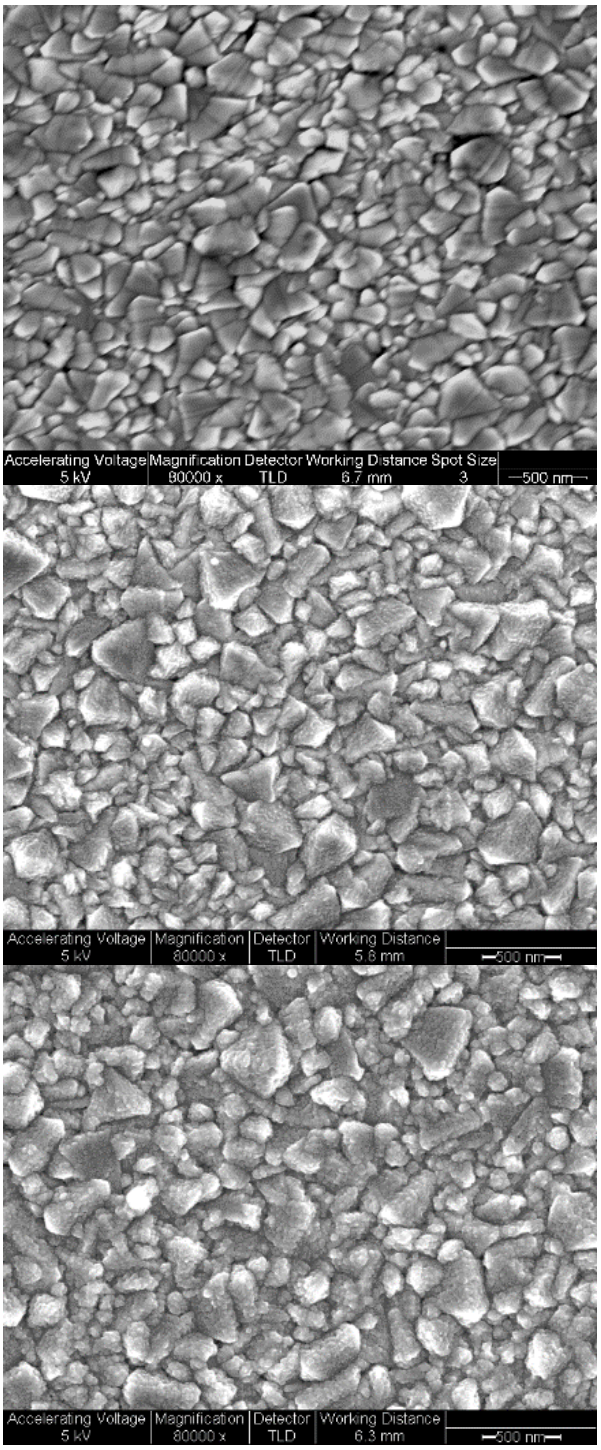

Figure S1. Top-view SEM images of bare FTO (top), CdS film on FTO using a 5 min deposition time (middle), and a 6 min deposition time (bottom), indicating a gradual increase in the thickness and coverage of the CdS films with time. At 5 min, the CdS films are mostly conformal, as evidenced by the increased roughness of the surfaces of the FTO crystallites, indicating growth of the CdS there, but occasional sharp edges indicative of the bare FTO surface remain. By 6 minutes, although the topography of the surface is similar to that of the bare FTO, the crystallite faces and edges alike are totally covered with the rough nanocrystalline material, indicating completely conformal coverage of the CdS.

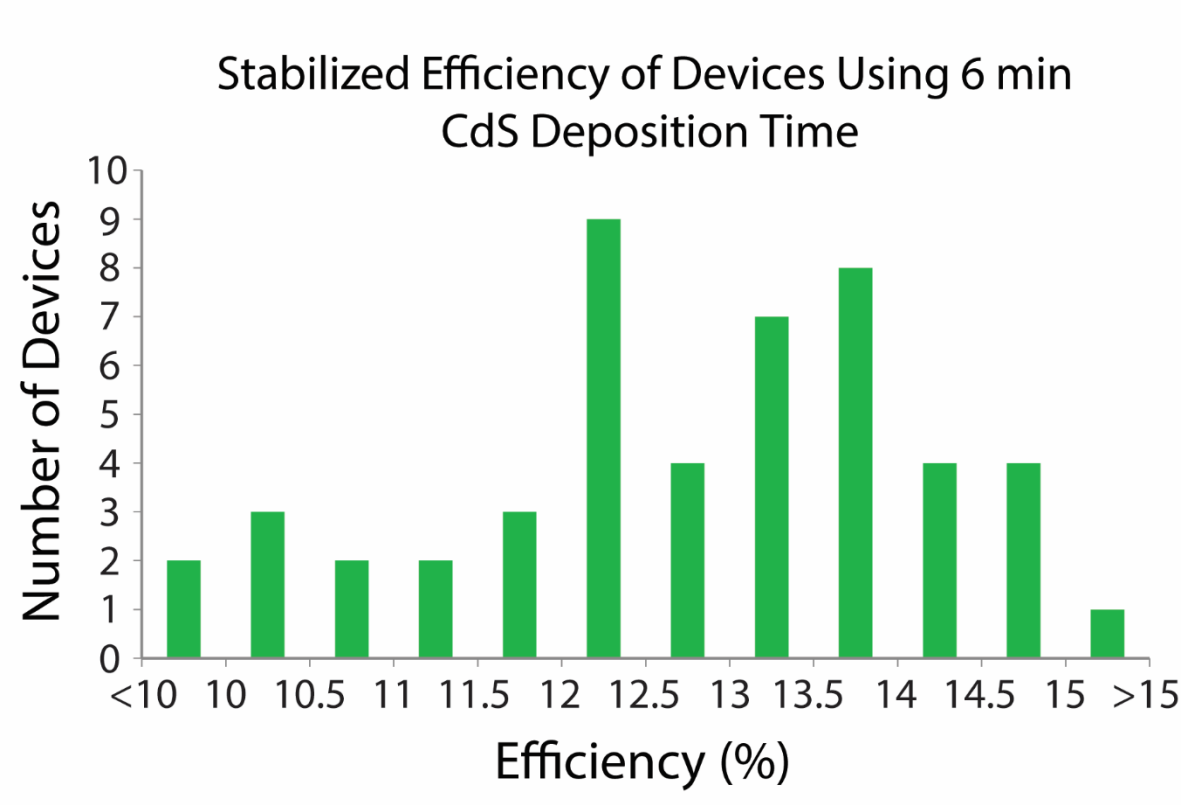

Figure S2. Histogram of stabilized efficiency of solar cells fabricated using 6 min CdS deposition time.

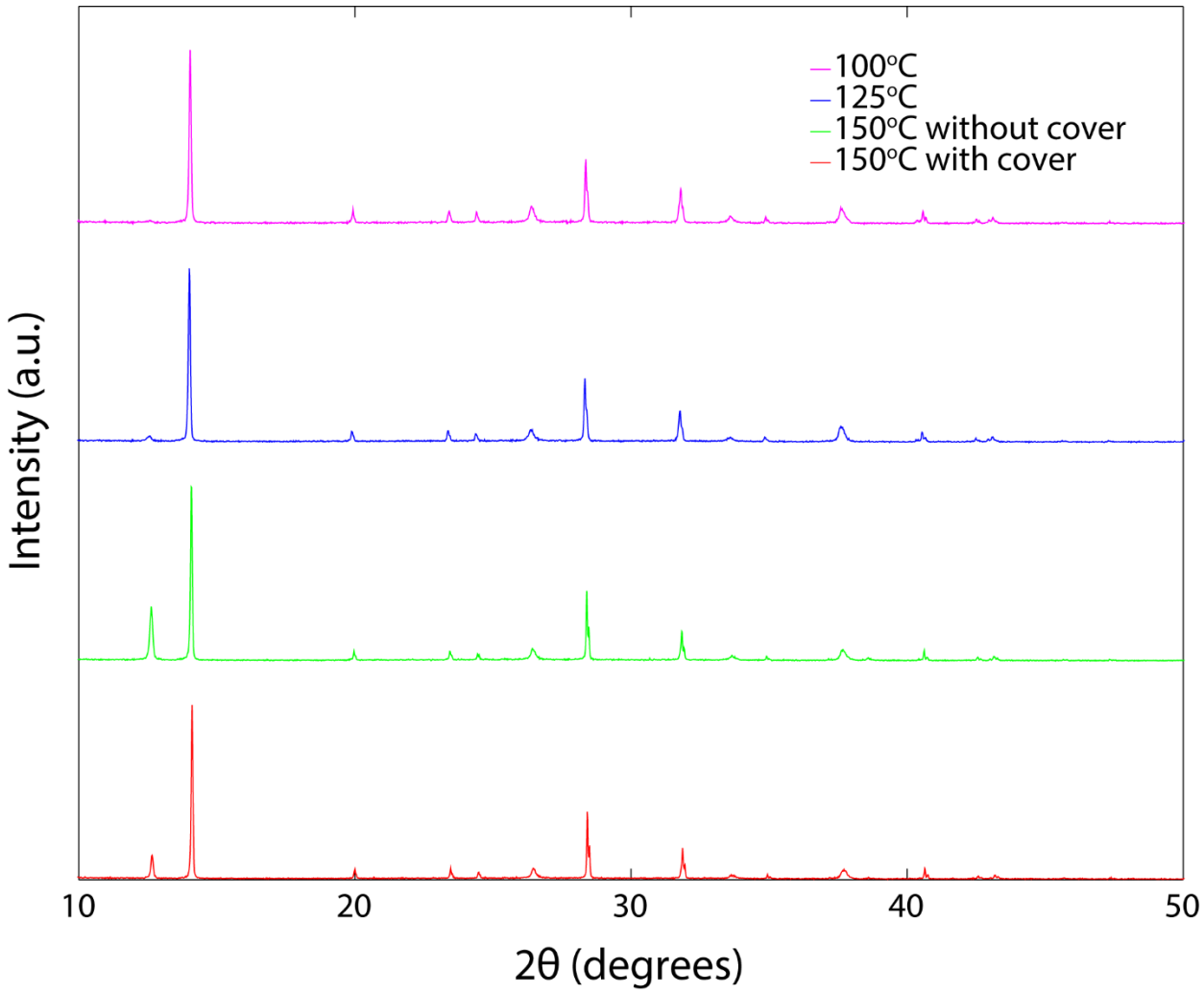

Figure S3. XRD patterns of perovskite on CdS annealed at different temperatures. The peak at ~12.5° belonging to PbI_2 does not grow substantially when annealing temperature is increased from 100 to 125°C, but there is considerable growth with an increase of anneal temperature to 150°C, indicating decomposition of the perovskite. This decomposition may be mitigated by covering the perovskite film during the anneal to prevent loss of the volatile methylammonium iodide.

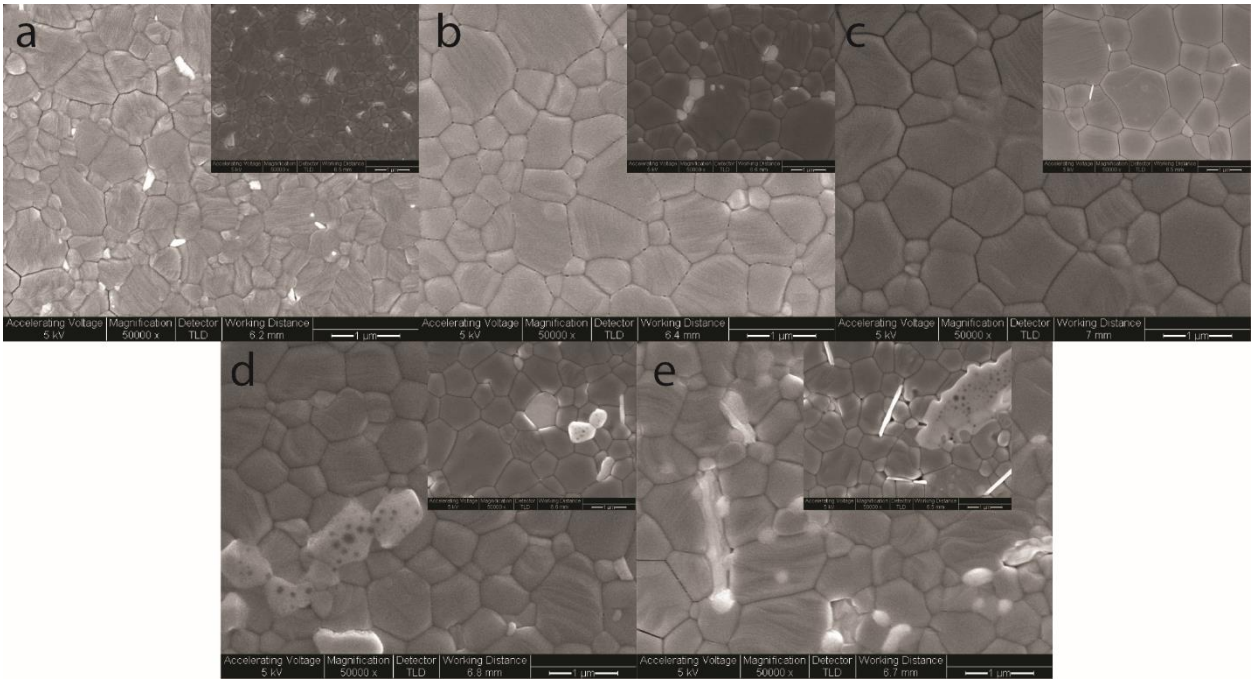

Figure S4. SEM images of Cd-containing perovskites fabricated on CdS (main images) and on glass (insets): a) undoped, b) 0.5% Cd, c) 1% Cd, d) 2% Cd, e) 5% Cd.

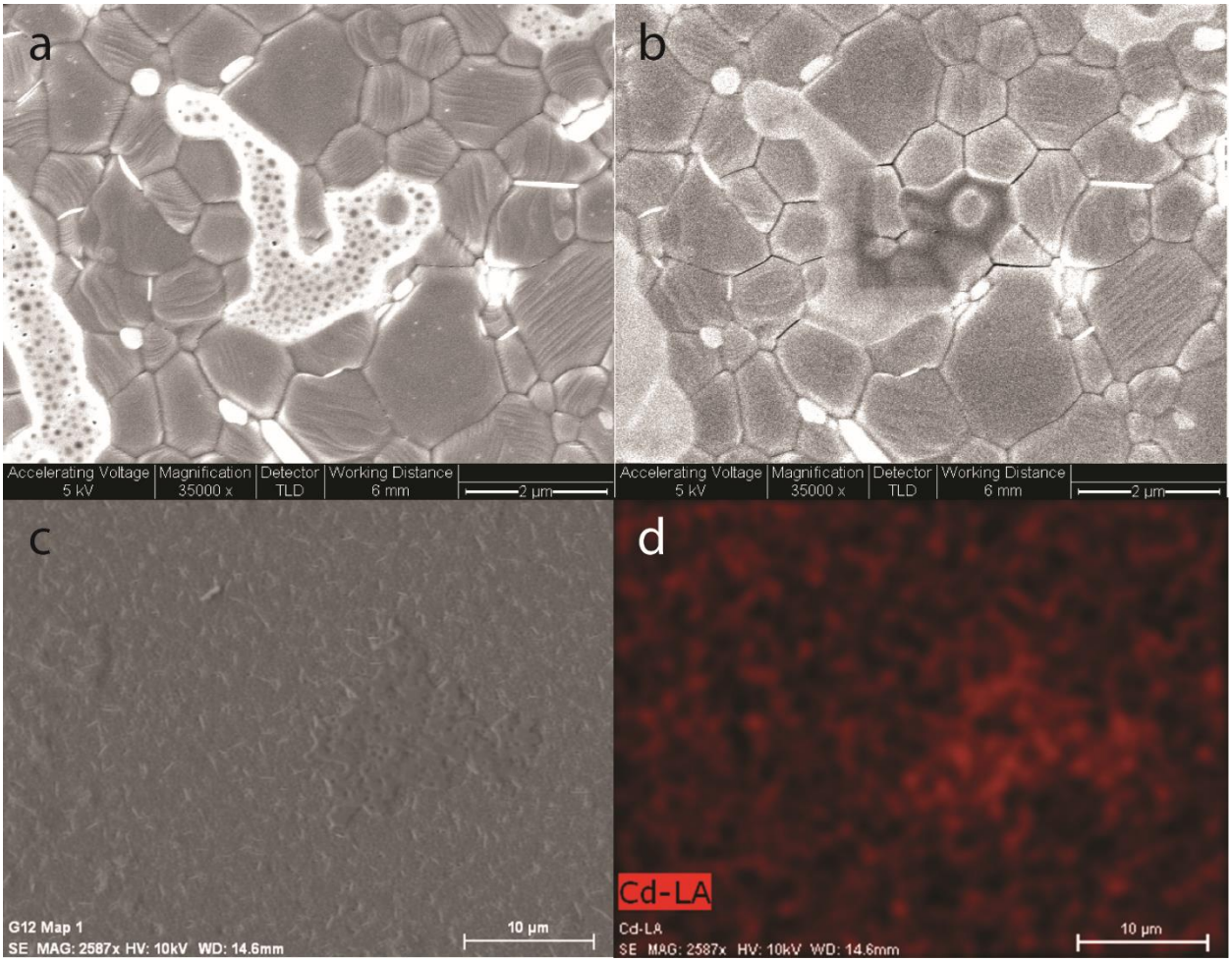

Figure S5. Etching of the blob-like secondary phase in the Cd-doped perovskite films. Panel a: initial SEM image of blob, which already exhibits some damage evident by the pattern of circular holes. Panel b: the same blob, after about a minute's exposure to the electron beam. The blob displays significant ablation, particularly in the center, where the beam was focused at higher magnification for several seconds. Panel c: low magnification SEM image of a region of secondary phase. Panel d: EDX map of the same region as c), showing enhancement of the Cd L-alpha emission.

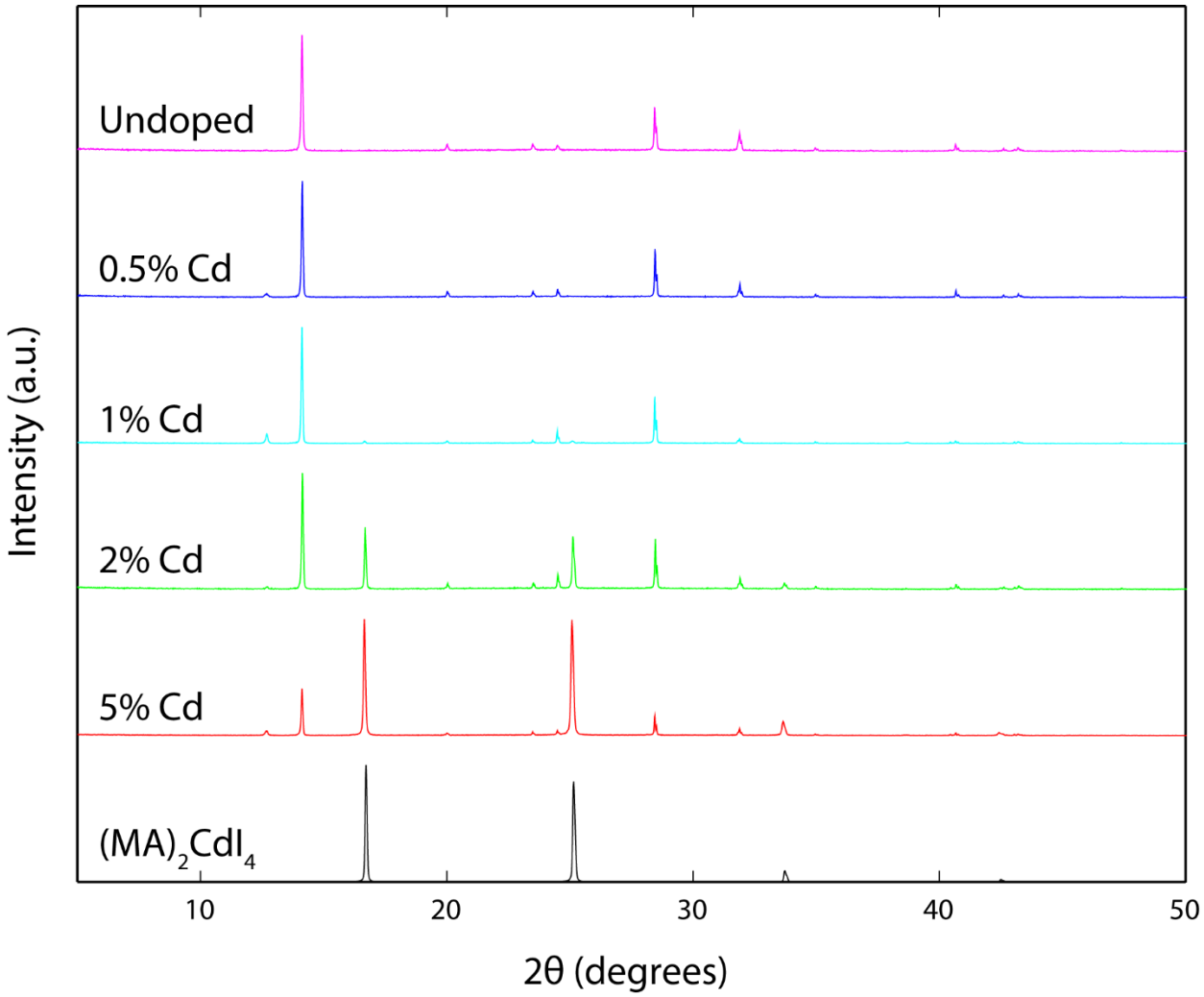

Figure S6. XRD patterns of the undoped and Cd-doped perovskites, compared against that of $(MA)_2CdI_4$. No $(MA)_2CdI_4$ peaks are evident in the 0.5% Cd films, but as Cd content in the precursor increases thereafter, the intensity of $(MA)_2CdI_4$ peaks increases, to the point at which these peaks dwarf those of the perovskite (perhaps due in part to preferred orientation for the $(MA)_2CdI_4$ materials).